coatings

MDPI

Article

Flexible Micro-Sensor Packaging and Durability for Real-Time Monitoring of Vanadium Flow Batteries

Chi-Yuan Lee [1,*], Chin-Lung Hsieh [2], Chia-Hung Chen [3], Lung-Jieh Yang [4], Ching-Liang Dai [5], Chong-An Jiang [1] and Yu-Chun Chen [1]

[1] Department of Mechanical Engineering, Yuan Ze Fuel Cell Center, Yuan Ze University, Taoyuan 32003, Taiwan
[2] Institute of Nuclear Energy Research, Taoyuan 325207, Taiwan
[3] HOMYTECH Global Co., Ltd., Taoyuan 33464, Taiwan
[4] Mechanical and Electromechanical Engineering, Tamkang University, Tamsui 251301, Taiwan
[5] Department of Mechanical Engineering, National Chung Hsing University, Taichung 402, Taiwan
* Correspondence: cylee@saturn.yzu.edu.tw

Abstract: The reactions of vanadium redox flow batteries (VRFBs) are quite complex and the internal environment is strongly acidic. The internal voltage, current, temperature and flow distribution play a very important role in the performance of a VRFB. The VRFB, which was developed by our R&D team, encountered easy leakage of electrolytes during assembly. Additionally, the strongly acidic environment can easily cause aging or failure of these VRFBs and of the micro-sensor. Therefore, this research was aimed at the need for real-time micro-diagnosis inside the VRFB. The use of micro-electro-mechanical systems (MEMS) technology was proposed so as to develop a flexible, integrated (current, voltage, flow and temperature), micro-sensor, and a durability test was conducted after packaging. Further, we performed real-time monitoring of the VRFBs. The main finding was that the encapsulation contributed to the stability of the micro-sensor without any failure due to excessive flow impacting the sensor. In the end we successfully used a 3D printed package to protect the micro-sensor.

Keywords: flexible integrated micro-sensor; vanadium flow battery (VRFB); micro-sensor packaging; durability test; micro-electro-mechanical systems

Citation: Lee, C.-Y.; Hsieh, C.-L.; Chen, C.-H.; Yang, L.-J.; Dai, C.-L.; Jiang, C.-A.; Chen, Y.-C. Flexible Micro-Sensor Packaging and Durability for Real-Time Monitoring of Vanadium Flow Batteries. *Coatings* **2022**, *12*, 1531. https://doi.org/10.3390/coatings12101531

Academic Editor: Emerson Coy

Received: 5 September 2022
Accepted: 11 October 2022
Published: 13 October 2022

1. Introduction

World power generation is currently very dependent on petroleum-based energy sources, such as liquid fuels, natural gas, and coal. There are two major problems with the use of these energy sources: one is that fossil fuels will have run out within the next 100 years, and the other is that carbon emissions and greenhouse gases (GHGs) adversely affect ecosystems. Human health and the living environment have been seriously threatened, so developed countries have formulated environmental protection regulations to reduce greenhouse gases. Renewable energy can simultaneously reduce greenhouse gas emissions and meet global energy needs.

Power storage devices are particularly important, among which the "vanadium flow battery" stands out among power storage devices. VRFBs are the most representative type of flow battery. Unlike previous battery systems, the positive and negative electroactive species in redox flow batteries are stored in tanks outside the stack. In this way, the power output and power storage capacity of the flow battery can be independently used to adapt to the required environment. For example, if applied to a battery with high energy storage, the amount of electroactive material in the tank can be increased to increase the energy storage effect, without major modifications to the battery stack. The electroactive material is placed in an external tank, so increasing the amount of electroactive material does not require changes to the stack. Such an approach enables changes to battery design to increase energy output at minimal cost, without impacting the battery's power output.

Conversely, if power must be maintained and the power delivered more efficiently, this usually results in a significant increase in cost. Therefore, the need to improve battery energy content requires increasing the amount of electroactive material in the outer canister without requiring major modifications to the stack in contrast to placing the electroactive material in the stack, which would increase the size of the battery pack and, thus, the cost [1–8].

In addition, during the VRFB operation, some vanadium ions diffuse through the membrane material, and this phenomenon causes loss of capacity of the battery and may also cause the temperature of the electrolyte to rise. According to the literature, the condition whereby vanadium ions gradually precipitate in the electrolyte in the form of pentavalent vanadium occurs when the temperature of the VRFB is higher than 40 °C. Precipitation of divalent and trivalent vanadium ions and deposition in the flow channel occurs when the temperature is lower than 10 °C, and this seriously affects the flow of the vanadium electrolyte, and can even cause the flow channel to block, which then causes the pump transporting the electrolyte to consume more power. Gundlapalli et al. compared different electrolyte flow rates and flow fields for VRFBs. When the flow rate was 1.2 mL/s, the performance of the VRFB without the flow field was better than that of the battery with the flow field. Yang et al. studied the effect of the pH value of the VRFB electrolyte on the voltage. From the experimental results, it was acknowledged that as the pH of both electrodes decreased, the cell voltage increased. Abbas and others found that the charge and discharge current densities of VRFB have a great influence on the charge and discharge efficiency, voltage efficiency and energy efficiency of VRFBs. Zeng et al. studied the charge–discharge and voltage changes of VRFBs under different currents. They found that the higher the current density, the shorter the charging and discharging time, and the closer the curve was to linear. The important advantages of VRFBs include the following: non-flammability, good stability, long running time, easy regeneration or recycling of the electrolyte, a long cycle life, amongst others. The disadvantage is that the energy density is low (weight and volume), so mobile applications are not often seen on the market, and they are relatively expensive, compared to lithium-ion batteries. The high cost is mainly because maturity of the product is not high, and there is no mass production [9–15].

When the VRFB energy storage system works at normal temperature and pressure, the electrolyte can effectively discharge the heat generated by the battery system, and then release it to the outside of the system through thermal convection. The electrolyte is a non-explosive and non-flammable aqueous solution with high safety. The charging and discharging of the VRFB energy storage system mainly utilizes the redox reaction of the yin and anode of the battery. Vanadium ions have four valence states which can exist stably: +2, +3, +4, and +5. Electrical energy is generated by chemical energy utilizing the flow cycle of electrolytes through redox processes of the active materials [16–23].

According to Huang express, an inductive proximity sensor with a 3D printed ceramic housing and an embedded sensing element was designed and produced using a hybrid manufacturing process, where the sensing element was embedded in the printed structure and the printing process paused. The conclusion was that the sensing element remained functional during every manufacturing process and demonstrated the ability of a fully encapsulated sensor to function at high temperatures. At a frequency of 2 MHZ and a voltage of 1 V, the measuring range of the inductive sensor was about 7.0 mm [24].

The packaging of tiny sensors is more complex than electronics. Electronic packages tend to provide environmental isolation, mechanical protection, and heat dissipation, while tiny sensors interact with the outside world to some extent, and fragile sensing chips or actuators need to be tested for exposure to the medium they operate in. All media adversely affect the tiny sensors, so micro-sensor packaging tends to be a highly specialized application. The same micro-sensor may have different packaging methods, due to different applications. Therefore, micro-sensor packaging is more challenging than electronic packaging. In addition to the basic function of electronic packaging, there is a need to avoid unnecessary contamination or reaction of the device materials with the

environment, especially in biomedical, pharmaceutical, and food applications. There is currently no general encapsulation method for micro-sensor packaging. The same micro-sensor may have different packaging methods due to different applications. Therefore, the micro-sensor packaging process cannot be standardized, and it is difficult to reduce the cost. Over the years, the packaging and testing of micro-sensors has accounted for 50%–90% of the cost of the entire micro-sensors. Therefore, both industry and academia are researching solutions to the problems.

Since the internal environment of a VRFB is strongly acidic, aging or failure of the micro-sensor are likely. Therefore, in this study, the micro-sensor was packaged and tested for durability, and then it was practically applied to real-time monitoring of a VRFB.

First, you need to understand the internal environment and requirements of the battery, then you need to design the sensor package, use 3D printing technology to print the packaged shell and then, in the experimental part, you need to calibrate the sensor to see if the data is normal. Finally, the battery's experimental results are measured. The packaged micro-sensors are mainly placed at the inlet and outlet of the electrolyte tank of the large vanadium redox flow battery energy storage system, while the unpackaged micro-sensors are embedded inside the battery [25].

2. Process and Packaging of Micro-Sensor

Firstly, the flexible integrated (voltage, current, temperature and flow) micro-sensor made by our laboratory [25] was used for package design, fabrication and durability testing, and then practically applied to real-time monitoring of a VRFB. Detailed specifications of the flexible integrated micro-sensor follow.

There are two types of package designs for the flexible integrated micro-sensor. The overall length is 90 mm, the diameter is 30 mm, and the front end is placed in a pipeline of about 25 mm. The first design has no front and only the sensor head is exposed, and the second design has a reduced 10 mm front opening. Then, 3D printing was used to produce the housings of the two micro-sensors (Figure 1).

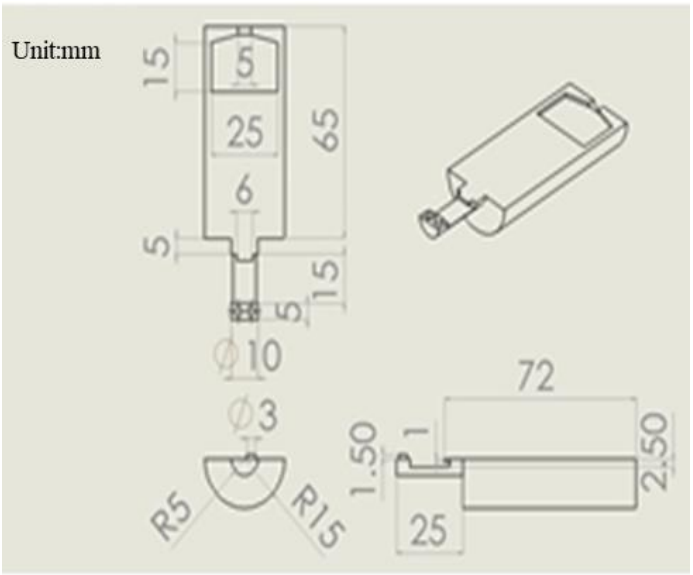

Figure 1. *Cont.*

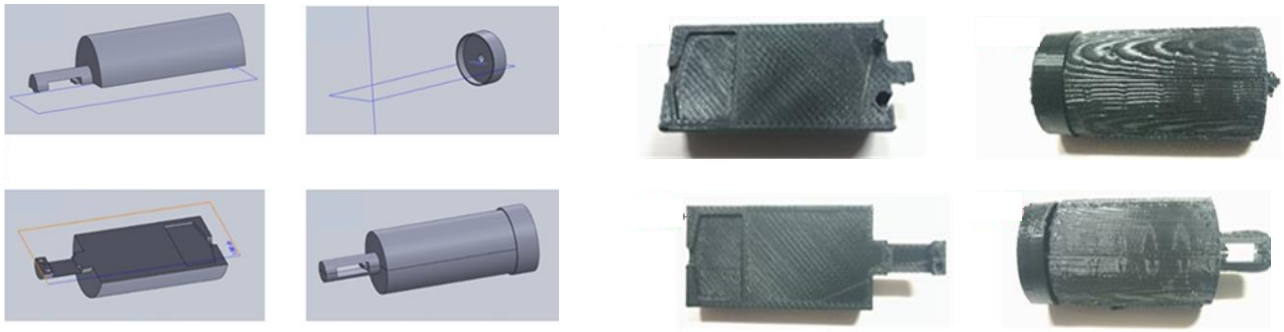

Figure 1. Image of 3D printed shell of micro-sensor.

3. Packaging and Endurance Testing of Micro-Sensor

After completing the 3D printing of the micro-sensor housing, the material of which was ABS (Acrylonitrile Butadiene Styrene), the packaging and durability tests were conducted.

3.1. Micro-Sensor Housing Processing

Since a violent electrochemical reaction occurs when the VRFB is charged, and the electrolyte is sulfuric acid, a layer of protective glue (Epoxy) was first applied to the shell of the micro-sensor. Then it was soaked in epoxy resin so as to withstand voltage and resistance, grinding, and acid and alkali resistance, as well as providing a seamless, beautiful, and easy to clean exterior, among other advantages. The final product is shown in Figure 2. Figure 3 shows the micro-sensor housing when processed. The micro-sensor was then packaged, as shown in Figure 4.

Figure 2. Micro-sensor housing after soaking.

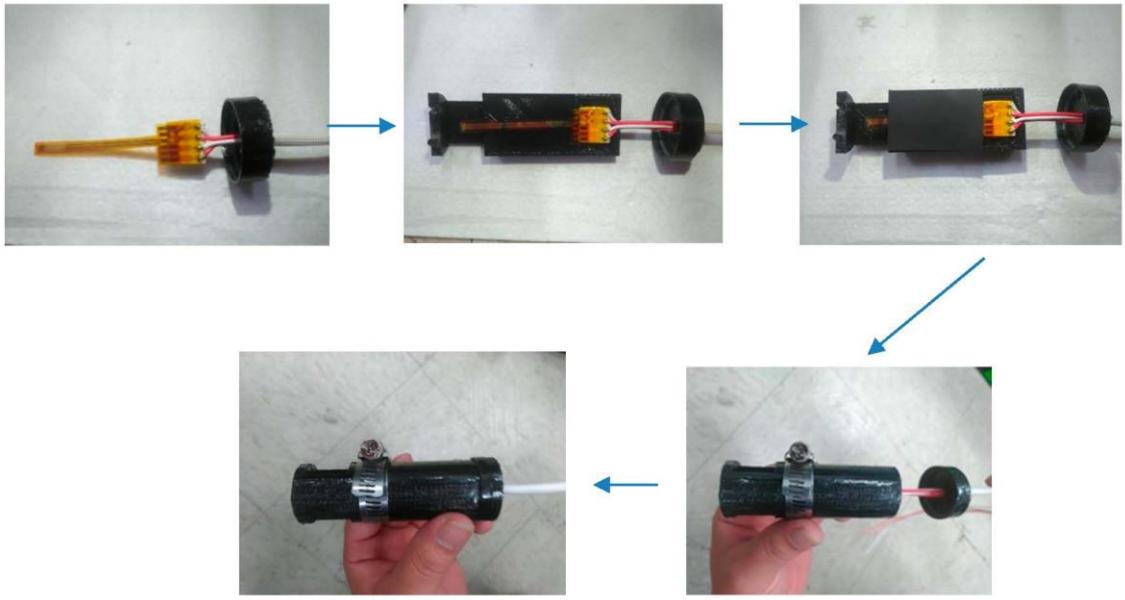

Figure 3. Packaging step.

Figure 4. Image of finished product after packaging.

3.2. Testing of Micro-Sensor Finished Product

3.2.1. Corrosion Resistance Test of Housing

In order to compare the anti-corrosion effect of the protective glue on the micro-sensor shell before and after, we took a casing with protective glue and a casing without a protective layer, and immersed the casings in vanadium electrolyte. The surface of the

casing without a protective film softened (Figure 5 left hand side), but the casing with the upper protective film remained the same (Figure 5 right hand side).

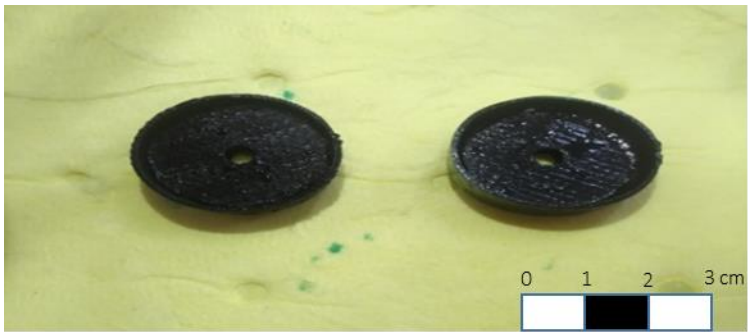

Figure 5. After immersing into the electrolyte.

3.2.2. Tightness Test of the Shell

The packaged micro-sensor product was immersed in vanadium electrolyte, and whether the inside of the micro-sensor was infiltrated by electrolyte was observed. Finally, the micro-sensor was disassembled after immersion, and there was no evidence of infiltration of vanadium electrolyte, as shown in Figure 6. The image on the left is of the outside, and that of the right the inside.

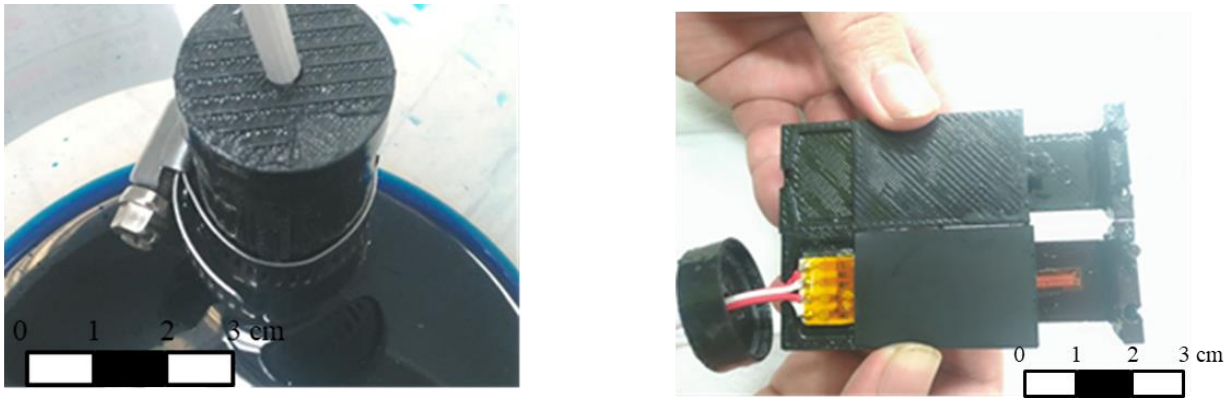

Figure 6. Tightness test.

3.3. Micro-Sensors Embedded in Vanadium Flow Batteries for Durability and Corrosion Tests

The first-stage of charging used the ABM series programmable power supply (PS9610A), as shown in Figure 7. The LabVIEW program could instantly capture the overall charging status of the vanadium flow battery and set the upper and lower limits of the charging cut-off. In the future, the program could be used to control the charging procedure of the vanadium redox flow battery. The second stage was the discharging procedure. In this study, the 3311F DC load from Prodigit Electronics Co., Ltd. (New Taipei City, Taiwan) was used, as shown in Figure 8. This model could be programmed through LabVIEW, with real-time capture of the overall discharge status of the vanadium flow battery and setting of the upper and lower limits of the discharge cut-off. In the future, the discharge procedure of the vanadium flow battery could be controlled by a program. In our current research, we selected the programmable control constant temperature and humidity testing machine (Hongda HT-8045A environmental test chamber, Taipei, Taiwan, Figure 9) as the benchmark for the calibration environment, and the data acquisition equipment used was NI PXI 2575 (Hsinchu, Taiwan, Figure 10). LabVIEW system design software and control system for signal processing and analysis was also used. Finally, the analyzed and processed data was processed by the computer to draw the calibration curves. Figures 11 and 12 are calibration curves of flow rate and temperature of the

micro-sensors. After the micro-sensor was manufactured, it was embedded in the VRFB (Figure 13) for testing, and then the micro-sensor was connected to the instrument to read data. The data was read while the battery was charging, and actually obtained the runner voltage, current, temperature and flow data (Figures 14–17). This meant that the sensor was functioning normally when the battery was running.

Figure 7. ABM Series Programmable Controlled Power Supply.

Figure 8. 3311F DC Load.

Figure 9. Hung ta HT-8045A Environmental Chamber.

Figure 10. NI PXI 2575.

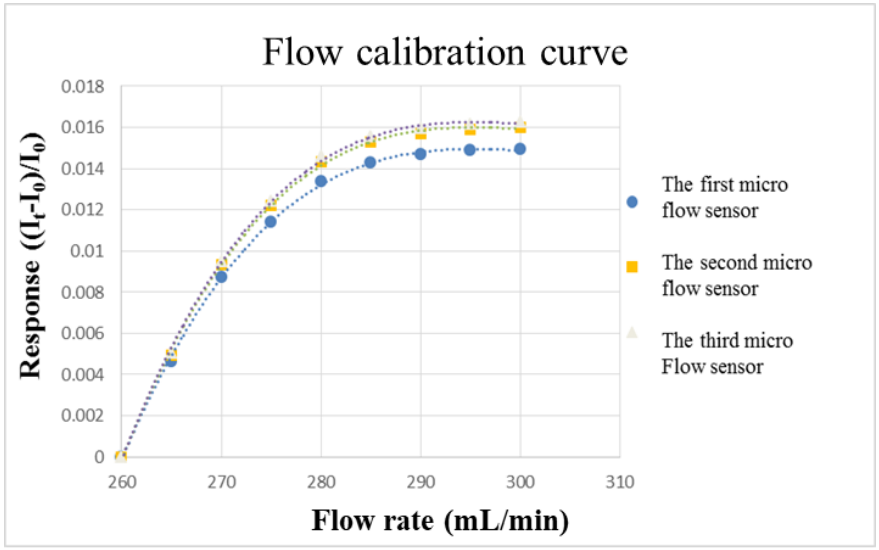

Figure 11. Flow calibration curve.

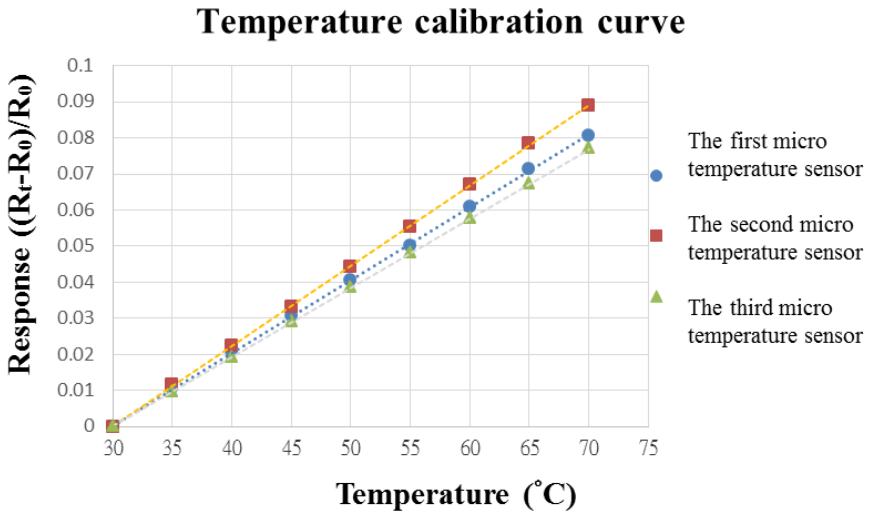

Figure 12. Temperature calibration curve.

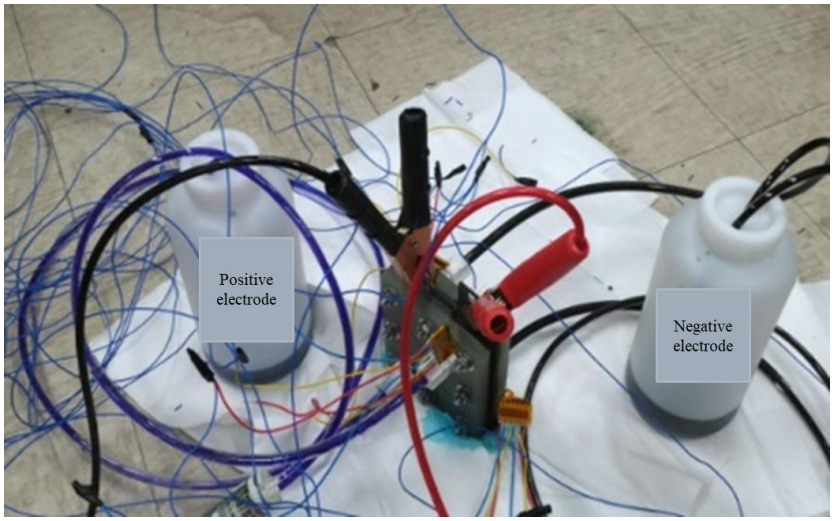

Figure 13. Charging diagram of micro-sensor embedded in VRFB.

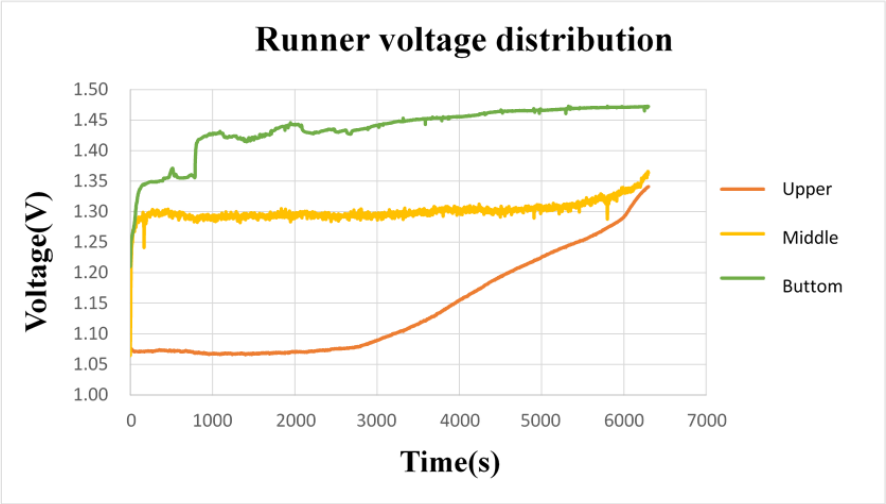

Figure 14. Runner voltage curve.

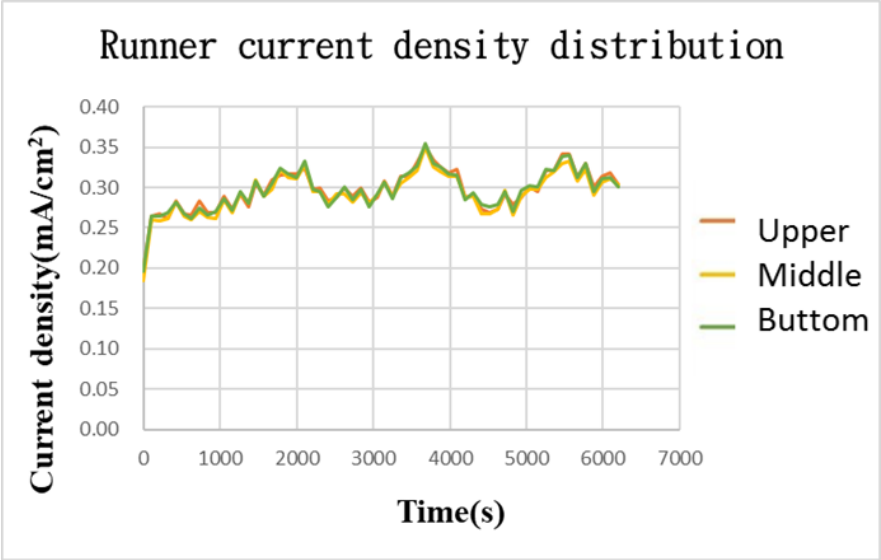

Figure 15. Runner current density curve.

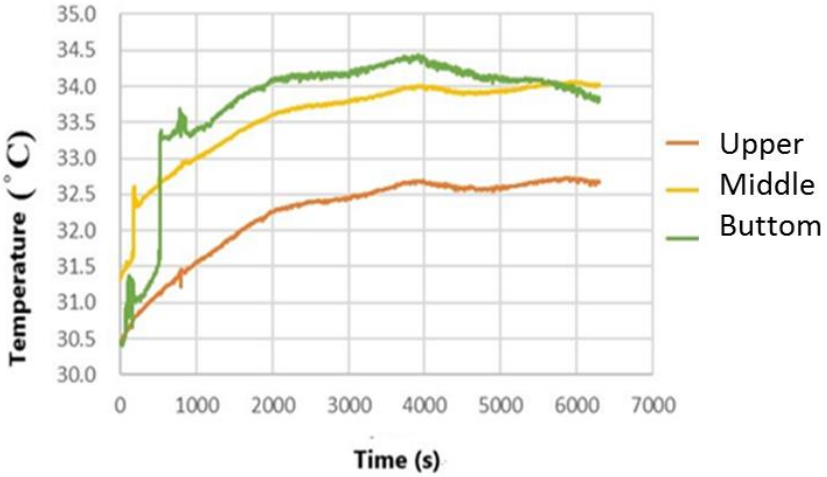

Figure 16. Runner charging temperature curve.

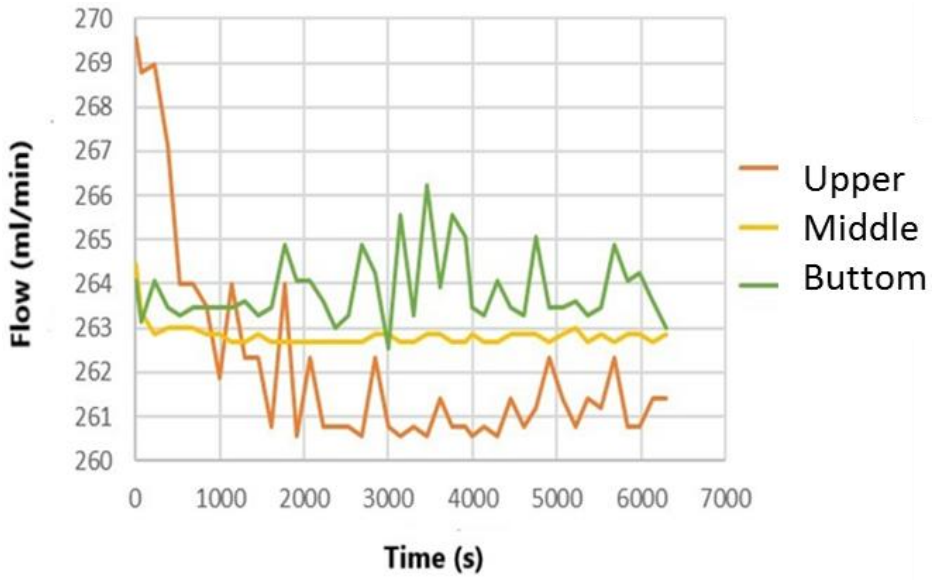

Figure 17. Runner flow distribution curve.

At the same time, when the micro-sensor was embedded in the VRFB test, the corrosion resistance and durability tests of the micro-sensor were simultaneously carried out. The micro-sensor was immersed in the vanadium electrolyte, and the value of resistance changed in the electrolyte (Figure 18). It can be seen from the data measurements with the NI PXI 2575 (Figure 10) that the micro-sensor could still be used normally after 624 h.

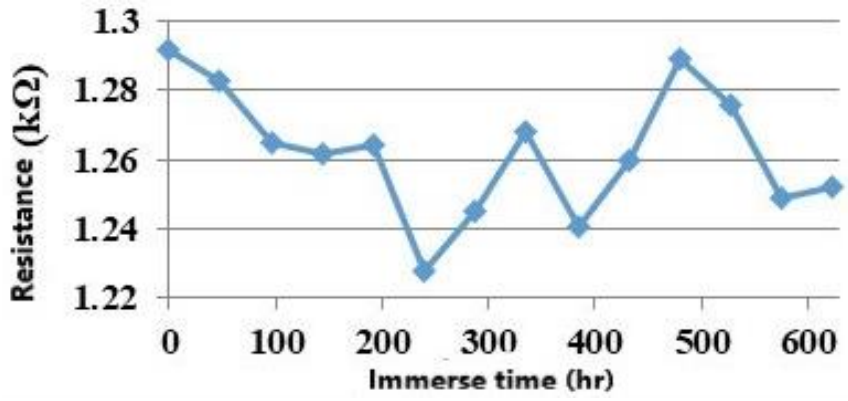

Figure 18. Resistance and the immerse time inside the electrolyte.

4. Conclusions

In this study, using MEMS technology, we successfully integrated micro-voltage, current, temperature and flow sensors on a polyimide film (PI) substrate, with a thickness of 50 μm. The electrochemical environment's corrosion resistance and acid resistance were selected. Polyimide (Fujifilm Durimide® PI7320) was used as a protective layer. This flexible, integrated, micro-sensor has four sensing functions, is thin with a small structural area, has high sensitivity, provides real-time measurement and can be placed in any position, among many other advantages. Both the micro-sensor itself and the package casing were tested for durability and corrosion resistance. The experimental results confirmed that its reliability and durability are good, and the real response information of the VRFB can be measured in real time. Facts proved that we successfully used 3D printing technology to create a package that can protect the sensor, and can also be replaced with different packages, according to different environments, which is quite an innovative idea and is also very economical.

Author Contributions: The work presented here was carried out in collaboration between all authors. C.-Y.L., C.-L.H., C.-H.C., L.-J.Y. and C.-L.D. conceived, designed, and discussed this study C.-A.J. and Y.-C.C. performed the experiments and analyzed the data. All authors have read and agreed to the published version of the manuscript.

Funding: The authors are grateful to the Ministry of Science and Technology of R.O.C. through the grant MOST 110-2221-E-155-034, 110-2221-E-155-061, 111-2622-E-155-006, 111-2622-8-155-004-TM and Institute of Nuclear Energy Research of R.O.C. through grants NL 1070289, 1061191, 1050770, 1040734.

Acknowledgments: The authors would also like to thank the HOMY Technology, YZU Fuel Cell Center and NENS Common Lab, for providing access to their research facilities.

Conflicts of Interest: The authors declare no conflict of interest.

References

1. Rahman, M.; Oni, A.O.; Gemechu, E.; Kumar, A. Assessment of energy storage technologies: A review. *Energy Convers. Manag.* **2020**, *223*, 113295. [CrossRef]
2. Mutezo, G.; Mulopo, J. A review of Africa's transition from fossil fuels to renewable energy using circular economy principles. *Renew. Sustain. Energy Rev.* **2021**, *137*, 110609–110623. [CrossRef]
3. Nair, S.; Timms, W. Freshwater footprint of fossil fuel production and thermal electricity generation and water stresses across the National Electricity Market (NEM) region of Australia. *J. Clean. Prod.* **2020**, *267*, 122085. [CrossRef]
4. Nong, D.; Simshauser, P.; Nguyen, D.B. Non-CO_2 greenhouse gases and climate change. *Nature* **2021**, *476*, 11723–11733.
5. Ashfaq, S.; Tang, Y.; Maqbool, R. Volatility spillover impact of world oil prices on leading Asian energy exporting and importing economies' stock returns. *Energy* **2019**, *188*, 116002. [CrossRef]
6. Clerides, S.; Krokida, S.I.; Lambertides, N.; Tsouknidis, D. What matters for consumer sentiment in the euro area? World crude oil price or retail gasoline price? *Energy Econ.* **2022**, *20*, 105743–105753. [CrossRef]
7. Skea, J.; Diemen, R.V.; Pereira, J.P.; Khourdajie, A.A. Outlooks, explorations and normative scenarios: Approaches to global energy futures compared. *Technol. Forecast. Soc. Chang.* **2021**, *168*, 120736–120754. [CrossRef]
8. Manohar, A.K.; Kim, K.M.; Plichta, E.; Hendrickson, M.; Rawlings, S.; Narayanan, S.R. A High Efficiency Iron-Chloride Redox Flow Battery for Large-Scale Energy Storage. *J. Electrochem. Soc.* **2015**, *163*, A5118–A5125. [CrossRef]
9. Alphonse, P.-J.; Elden, G. The investigation of thermal behavior in a vanadium redox flow battery during charge and discharge processes. *J. Energy Storage* **2021**, *40*, 102770. [CrossRef]
10. Huang, Z.; Mu, A.; Wu, L.; Wang, H.; Zhang, Y. Electrolyte flow optimization and performance metrics analysis of vanadium redox flow battery for large-scale stationary energy storage. *Int. J. Hydrogen Energy* **2021**, *46*, 31952–31962. [CrossRef]
11. Gundlapalli, R.; Jayanti, S. Effect of channel dimensions of serpentine flow fields on the performance of a vanadium redox flow battery. *J. Energy Storage* **2019**, *23*, 148–158. [CrossRef]
12. Yang, W.; He, Y.; Li, Y. Performance Modeling of a Vanadium Redox Flow Battery during Discharging. *Electrochim. Acta* **2015**, *155*, 279–287. [CrossRef]
13. Abbas, Q.; Mirzaeian, M.; Gibson, D. Vanadium Air/Redox Flow Batteries. *Encycl. Smart Mater.* **2021**, *2*, 198–207. [CrossRef]
14. Zeng, Y.; Zhao, T.; An, L.; Zhou, X.; Wei, L. A comparative study of all-vanadium and iron-chromium redox flow batteries for large-scale energy storage. *J. Power Sources* **2015**, *300*, 438–443. [CrossRef]
15. Doetsch, C.; Burfeind, J. 17—Vanadium redox flow batteries. In *Storing Energy*, 2nd ed.; with Special Reference to Renewable Energy Sources; Elsevier: Amsterdam, The Netherlands, 2022; pp. 363–381.
16. Mehrjerdi, H. Dynamic and multi-stage capacity expansion planning in microgrid integrated with electric vehicle charging station. *J. Energy Storage* **2020**, *29*, 101351. [CrossRef]
17. Shang, Y.; Wu, W.; Guo, J.; Ma, Z.; Sheng, W.; Lv, Z.; Fu, C. Stochastic dispatch of energy storage in microgrids: An augmented reinforcement learning approach. *Appl. Energy* **2020**, *261*, 114423. [CrossRef]
18. Ranjan, M.; Shankar, R. A literature survey on load frequency control considering renewable energy integration in power system: Recent trends and future prospects. *J. Energy Storage* **2021**, *45*, 103717. [CrossRef]
19. Yu, Z.; Lu, F.; Zou, Y.; Yang, X. Quantifying energy flexibility of commuter plug-in electric vehicles within a residence–office coupling virtual microgrid. Part I: System configuration, quantification framework, and optimization model. *Energy Build.* **2022**, *254*, 111551–111563. [CrossRef]
20. Liu, L.; Wang, C.; He, Z.; Das, R.; Dong, B.; Xie, X.; Guo, Z. An overview of amphoteric ion exchange membranes for vanadium redox flow batteries. *J. Mater. Sci. Technol.* **2021**, *69*, 212–227. [CrossRef]
21. Kazacos, M.; Cheng, M. Vanadium redox cell electrolyte optimization studies. *J. Appl. Electrochem.* **1990**, *20*, 463–467. [CrossRef]
22. Liu, T.; Li, X.; Zhang, H.; Chen, J. Greenhouse gas emissions vs. CO_2 emissions: Comparative analysis of a global carbon tax. *Appl. Energy* **2018**, *298*, 1292–1303. [CrossRef]
23. Duan, Z.; Qu, Z.; Wang, Q.; Wang, J. Structural modification of vanadium redox flow battery with high electrochemical corrosion resistance. *Appl. Energy* **2019**, *250*, 1632–1640. [CrossRef]

24. Huang, R.; Urban, A.; Jiao, D.; Zhe, J.; Choi, J.-W. Inductive proximity sensors within a ceramic package manufactured by material extrusion of binder-coated zirconia. *Sens. Actuators A Phys.* **2022**, *338*, 113497–113508. [CrossRef]
25. Lee, C.-Y.; Lee, S.-J.; Chen, C.-H.; Hsieh, C.-L.; Wen, S.-H.; Chiu, C.-W.; Jiang, C.-A. Internal real-time microscopic diagnosis of vanadium redox flow battery. *Sens. Actuators A Phys.* **2020**, *314*, 112259. [CrossRef]